ELSEVIER

Journal of Chromatography A, 764 (1997) 309–321

JOURNAL OF CHROMATOGRAPHY A

Separation power of isotachophoresis (displacement electrophoresis) with continuous pH and conductivity gradients[1]

K. Šlais

Institute of Analytical Chemistry, Academy of Sciences of the Czech Republic, Veveří 97, 611 42 Brno, Czech Republic

Accepted 21 October 1996

Abstract

Previous simple models of electrofocusing in a continuous pH gradient are extended to also cover changes in conductivity. The variance of a Gaussian zone is discussed to illustrate the impact of the conductivity gradient on the steady-state resolution and the peak capacity. The particular equations are used to compare the separation power of focusing in pH and/or the conductivity gradient for good and poor ampholytes as well as for weak and strong electrolytes. It was found that the resolution and the peak capacity in displacement electrophoresis with a continuous conductivity gradient can be comparable to that of focusing in a pH gradient and to the separation power of zone electrophoresis.

Keywords: Isotachophoresis; Displacement electrophoresis; Isotachophoretic focusing; Conductivity gradients; pH gradients

1. Introduction

Isotachophoresis (ITP) [1–5] (displacement electrophoresis, DE, [6–8]) is usually understood as the separation electrophoretic method in which the separated ionic solutes are detected as steady-state zones with a nearly square wave concentration profile. The ability of ITP to substantially increase the concentration of analytes in the steady-state focused zones relative to their concentration in the sample was demonstrated, e.g., in numerous variants of the combination of ITP with capillary zone electrophoresis (CZE) which were reviewed recently [9]. The focusing effect of ITP can be further increased when the capillary diameter for ITP preconcentration has a wider diameter than the capillary in which zone electrophoresis takes place [10–13].

It was shown [14] that some modes of electrofocusing, including isoelectric focusing (IEF) with electrophoretic mobilization [15–18], have certain features similar to ITP with the use of carrier ampholytes [1,19–22] and DE with carriers [8]. In all methods mentioned, the carriers generate the approximately linear pH gradient in which the analytes are focused into the Gaussian peaks. Based on the simplified models [23–25], the calculations of the peak width use the approximation of the constant conductivity along the pH gradient. Such an approximation was also used in the models of pH gradient which moves in the uniform [14] and the tapered [26–28] capillary. However, it is well known [1,19–22] that a considerable gradient of field strength and thus a gradient of conductivity (or resistivity) occurs in the pH gradient generated by isotachophoretic moving of the stack of carriers. The field strength increases approximately linearly from the leading end of the moving pH gradient toward the terminating end by up to one order of magnitude [1,20]

[1]Presented at the 10th International Symposium on Advances and Applications of Chromatography in Industry, Bratislava, June 30–July 4, 1996.

PII S0021-9673(96)00902-8

or a hyperbolic decrease of the conductivity of the same magnitude was found in ITP with carrier ampholytes on gel slabs [19]. Further, it was demonstrated [21] that nucleotides and DNA fragments could be focused in the moving stack of carriers under conditions where an influence of pH gradient was rather limited. Charlionet et al. [29] introduced isotachophoretic focusing (ITF), as a method of separation of proteins characterized by a stable field strength gradient due to a continuous mobility spectrum which was claimed as a basic difference from IEF where ampholytes are focused in the pH gradient with a constant field strength. Though the equations derived for ITF [29] may be applicable to the background with constant pH, the accompanying experiments were carried in polyampholyte background where both pH and field strength gradients were generated. In order to come closer to reality, it is necessary to include the influence of both pH and the conductivity gradients in the theoretical estimation of the separation power of electrofocusing in continuous gradients. Further, it seems reasonable to examine the resolving power of the focusing of the strong and weak electrolytes into the Gaussian zones in the conductivity gradient with constant pH.

In the present contribution, the previous model [26–28] is modified to obtain the more general equation for calculation of the steady-state width of the Gaussian zone in the focusing modes of electrophoresis. It is applied to the focusing of the ampholytes as well as for the focusing of weak and strong electrolytes in the pH, conductivity and combined pH and conductivity gradients.

2. Theory

2.1. Steady-state peak variance

The simple models of focusing in a natural continuous pH gradient [23–25] involve the stack of great number of good ampholytes (carriers) which are focused into the Gaussian zones and separated so that the approximately linear pH gradient is formed. Due to the differences in their mobilities, the background ampholytes generate also stable field strength gradient under isotachophoretic conditions [29]. In Section 3.2, the possibility of the generation of combined pH and conductivity gradients in a background consisting of monoprotic weak or strong electrolytes is examined by computer modelling. The concentrations in the peak maxima, c_m, are substantially lower than the sum of concentrations of all carriers overlapping at a considered place of the stack. Since the zone width is inversely proportional to the field strength, E, the concentration in the peak maximum increases with E until it reaches the sum of concentrations of overlapping zones and the square wave profile develops [25,30]. When the stack is positioned between the leading electrolyte (LE) and the terminating electrolyte (TE), the sum of the concentrations of overlapping zones is adjusted to the concentration of LE. Then, the stack volume, V_g, can be regarded as constant when it moves in an uniform [14] as well in a nonuniform capillary [26–28] similarly to behavior of the single ITP zone. However, the actual zone width of an individual component is dependent on the local field strength, pH gradient and the departure from the local steady state [26–28]. The zone of analyte is considered to behave similarly as zones of carriers. However, when a suitable detection mode is chosen, it can be observed independently of carriers. Thus, within the limit of maintaining the Gaussian profiles of all zones, the stack of carriers can be treated as the continuum in which the analyte zone can be discussed independently of zones of carriers.

It was shown [31] that the diffusion and diffusion-like processes transform initial zones into the Gaussian zones in the majority of practical cases and the Gaussian function is the desired mathematical solution to the continuity equation. In the model described above, it was adopted that the changes in the environment which influence the shape of the concentration profile are such that the zone shape can be described in terms of a Gaussian curve. Thus, the zone variance can be treated as the variable in following treatment.

In the initial part of the theory, let us describe the influence of the local migration velocity, v, on the zone width as outlined in Fig. 1. The zone is regarded as that of an analyte or that of a background component. Since the local migration velocity can be regarded as uniform over the capillary cross section and the zone is close to the steady state, the radial concentration gradients can be neglected in com-

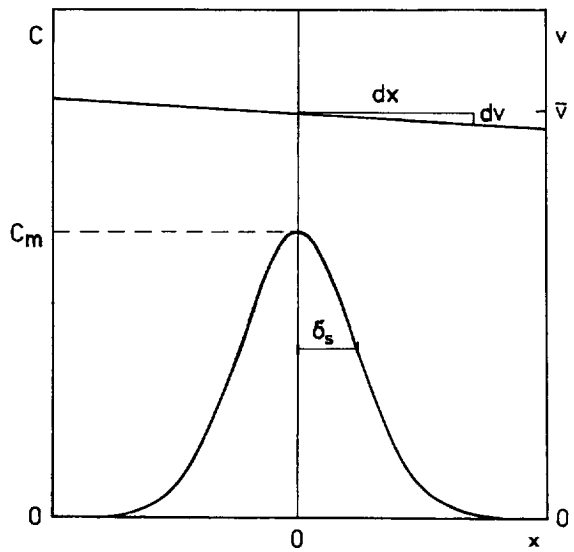

Fig. 1. Illustration of focusing in moving gradient of migration velocity. Symbols: x = moving length coordinate, the distance from peak center; σ_s = steady-state length based standard deviation of Gaussian zone; c = concentration; c_m = concentration in peak maximum; ν = local migration velocity of component; $\bar{\nu}$ = isotachophoretic velocity.

parison with the axial ones. When we accept the assumptions above, we can obtain the relation between the length based zone variance, σ^2, and the velocity gradient [26,28]:

$$\frac{D^* - D}{\sigma^2} = \frac{\mathrm{d}\nu}{\mathrm{d}x} \tag{1}$$

where $\mathrm{d}\nu/\mathrm{d}x$ is the gradient of the migration velocity along the zone, x is the length coordinate along the moving natural gradient with $x=0$ at the peak maximum, D is the diffusion coefficient and D^* is the effective dispersion coefficient. The migration velocity, ν, is the product of the effective mobility, μ, and the field strength, E

$$\nu = \mu E \tag{2}$$

and field strength is a function of electric current, I, conductivity, κ, and cross section, A:

$$E = \frac{I}{\kappa A} \tag{3}$$

Some derived equations can be simplified when we use the resistivity, ρ:

$$\rho = \frac{1}{\kappa} \tag{4}$$

In order to discuss the influence of the conductivity gradient on the Gaussian zone under the steady state, let us examine the displacement in the capillary of the constant cross section, which means $\mathrm{d}A/\mathrm{d}x = 0$. When the steady state is achieved, it is $\mathrm{d}\sigma^2/\mathrm{d}t = 0$ and $D^* = 0$. Then, the steady-state zone variance, σ_s^2, is from Eq. (1):

$$\sigma_s^2 = \frac{D}{-\mathrm{d}\nu/\mathrm{d}x} \tag{5}$$

and with Eqs. (2–4):

$$\frac{\mathrm{d}\nu}{\mathrm{d}x} = \nu \cdot \frac{\mathrm{d}\ln\mu}{\mathrm{d}x} + \nu \cdot \frac{\mathrm{d}\ln\rho}{\mathrm{d}x} \tag{6}$$

Since the shallow gradient of the migration velocity is assumed within the zone, and A is constant, it is reasonable to approximate ν in the second term on the right-hand side of Eq. (6) by the isotachophoretic velocity, $\bar{\nu} = \mathrm{d}y/\mathrm{d}t$ where y is capillary length coordinate. By insertion of Eqs. (2,6) in Eq. (5) we obtain the following for the steady-state peak variance with the last approximations:

$$\sigma_s^2 = \frac{-D}{\frac{\mathrm{d}\mu}{\mathrm{d}x} \cdot E + \bar{\nu} \cdot \frac{\mathrm{d}\ln\rho}{\mathrm{d}x}} \tag{7}$$

In the following paragraphs, the particular forms of the last equation are applied to the steady state in the continuous pH and conductivity gradients.

2.1.1. Peak variance in pH gradient with constant resistivity

For constant resistivity, $\mathrm{d}\rho/\mathrm{d}x = 0$ and we have the following from Eq. (7) for σ:

$$\sigma_s^2 = \frac{D}{\frac{-\mathrm{d}\mu}{\mathrm{d}x} \cdot E} \tag{8}$$

Thus, we have obtained the relation for the length based variance of the focused Gaussian zone of the good ampholyte under the steady state in the pH gradient as derived in the classical theory of IEF [23–25]. According to the Nernst–Einstein equation, the effective mobility is function of the effective charge, z, and D:

$$\mu = \frac{zFD}{RT} \tag{9}$$

In the pH gradient, z of the analyte is the function of local pH; the sensitivity of z to pH of the environment can be expressed in terms of $-\mathrm{d}z/\mathrm{d(pH)}$. The local steepness of pH gradient is usually expressed as the tangent, $\mathrm{d(pH)}/\mathrm{d}x$. Thus, the change in the mobility can be split into the term, which is characteristic for the analyte and to the term, which describes the separation medium and the geometry of the gradient. We can write:

$$\frac{\mathrm{d}\mu}{\mathrm{d}x} = \frac{\mathrm{d}z}{\mathrm{d(pH)}} \cdot \frac{\mathrm{d(pH)}}{\mathrm{d}x} \cdot \frac{FD}{RT} \tag{10}$$

where F, R, T have their usual meaning, see list of symbols (Section 5.1). By insertion of Eqs. (2–4,10) into Eq. (8) we obtain Eqs. (T1) in Table 1. The last equation can be used also for the pH gradient which moves in a capillary of constant cross section [14]. When biprotic poor ampholytes are focused in the pH gradient so that their mean effective charge, $\bar{z}$, is sufficiently different from zero, they can be treated as monoprotic weak electrolytes [14]. Then, $\mathrm{d}z/\mathrm{d(pH)}$ can be expressed in terms of $\bar{z}$ as:

$$\frac{-\mathrm{d}z}{\mathrm{d(pH)}} = 2.3\,\bar{z}\,(1-\bar{z}) \tag{11}$$

By insertion of Eq. (11) into Eqs. (T1) we obtain Eqs. (T2) in Table 1.

2.1.2. Peak variance in a resistivity gradient with constant pH

For constant pH, it follows from Eqs. (2–4,7):

$$\sigma_s^2 = \frac{D}{\frac{\bar{\mu}I}{A} \cdot \frac{-\mathrm{d}\rho}{\mathrm{d}x}} \tag{12}$$

This equation is similar to Eq. (4) in Ref. [29]. Eq. (12) can be applied for focusing of all electrolytes in a resistivity gradient with constant pH. With use of Eq. (9), Eq. (12) can be written as Eqs. (T3) in Table 1.

2.1.3. Peak variance in combined pH and resistivity gradients

Eq. (7) describes the influence of both pH and ρ gradients on the peak variance. Similarly to the above equations, it may be modified into the form:

$$\sigma_s^2 = \frac{D}{\frac{\bar{\rho}I}{A} \cdot \frac{-\mathrm{d}\mu}{\mathrm{d(pH)}} \cdot \frac{\mathrm{d(pH)}}{\mathrm{d}x} + \frac{\bar{\mu}I}{A} \cdot \frac{-\mathrm{d}\rho}{\mathrm{d}x}} \tag{13}$$

With use of the Nernst equation, we have:

$$\sigma_s^2 = \frac{-RT}{\frac{FI}{A}\left(\bar{\rho} \cdot \frac{\mathrm{d}z}{\mathrm{d(pH)}} \cdot \frac{\mathrm{d(pH)}}{\mathrm{d}x} + \bar{z}\frac{\mathrm{d}\rho}{\mathrm{d}x}\right)} \tag{14}$$

Here, $\bar{\rho}$ and $\bar{z}$ are the mean resistivity and the solute mean effective charge at the peak position within the stack, respectively. Since all variables in Eq. (14) can be regarded as constant while the stack moves within the capillary, the peak variance also remains constant.

2.2. Steady-state peak resolution

Peak resolution, R_s, was defined by Giddings [24,32] for description of the quality of the separation of two partially overlapping Gaussian peaks. When we use second subscript "s" for the indication of the steady-state resolution, R_{ss}, we can write:

$$R_{ss} = \frac{\Delta x_s}{4\sigma_s} \tag{15}$$

where Δx_s is the distance between centers of closely separated peaks. With use of the above relationships for σ_s in the discussed gradients, we can obtain the respective resolutions, see Table 1, second column.

2.2.1. Resolution in pH gradient with constant resistivity

For closely separated peaks in the pH gradient with constant ρ, the term is $\Delta\mathrm{(pH)}/\Delta x = \mathrm{d(pH)}/\mathrm{d}x$ and using Eqs. (8–10) we obtain:

$$R_{ss} = \frac{\Delta\mathrm{(pH)}}{4}\sqrt{\frac{(-\mathrm{d}z/\mathrm{d(pH)})FE}{(\mathrm{d(pH)}/\mathrm{d}x)RT}} \tag{16}$$

For the stationary pH gradient, when the pH of the focused zones equals the pI of the good ampholyte, we obtain the well known relation for estimation of resolution in IEF [23,24], see Eqs. (T4) in Table 1. As long as $\mathrm{d}z/\mathrm{d(pH)}$ terms of the two separated analytes are similar to each other, Eqs. (T4) holds

Table 1
Summary of equations for estimation of peak variance, resolution and peak capacity in moving continuous linear pH and resistivity gradients.

Conditions	Analytes	$\sigma_x^2 =$		$R_s =$		$n =$	
ρ = constant, d(pH)/dx ≠ 0	GA[a]	$\dfrac{RT}{\dfrac{\bar{\rho}FI}{A}\cdot\dfrac{\mathrm{d(pH)}}{\mathrm{d}x}\cdot\dfrac{-\mathrm{d}z}{\mathrm{d(pH)}}}$	(T1)	$\dfrac{\lvert\Delta(\mathrm{p}I)\rvert}{4}\sqrt{\dfrac{FE[-\mathrm{d}z/\mathrm{d(pH)}]}{RT[\mathrm{d(pH)}/\mathrm{d}x]}}$	(T4)	$\sqrt{\dfrac{FU_g\,\delta(\mathrm{pH})[-\mathrm{d}z/\mathrm{d(pH)}]}{16RT}}$	(T8)
ρ = constant, d(pH)/dx ≠ 0	WE, PA	$\dfrac{RT}{\dfrac{\bar{\rho}FI}{A}\cdot\dfrac{\mathrm{d(pH)}}{\mathrm{d}x}\cdot 2.3\lvert\bar{z}\rvert(1-\lvert\bar{z}\rvert)}$	(T2)	$\dfrac{\lvert\Delta(\mathrm{p}K_a)\rvert}{4}\sqrt{\dfrac{2.3\,FE\lvert\bar{z}\rvert(1-\lvert\bar{z}\rvert)}{RT[\mathrm{d(pH)}/\mathrm{d}x]}}$	(T5)	$\sqrt{\dfrac{FU_g\,\delta(\mathrm{pH})\lvert\bar{z}\rvert(\lvert\bar{z}\rvert-1)}{7RT}}$	(T9)
$\mathrm{d}\rho/\mathrm{d}x \neq 0$ pH = constant	SE, WE, GA, PA,	$\dfrac{RT}{\dfrac{\bar{z}FI}{A}\cdot\dfrac{-\mathrm{d}\rho}{\mathrm{d}x}}$	(T3)	$\dfrac{\Delta\mu}{4\bar{\mu}}\sqrt{\dfrac{\bar{z}F\bar{E}\bar{\rho}}{RT(-\mathrm{d}\rho/\mathrm{d}x)}}$	(T6)	$\sqrt{\dfrac{-\bar{z}FU_g}{8RT}}$	(T10)
ρ = constant, pH = constant	SE, WE, GA, PA	∝		$\dfrac{\Delta\mu}{4\bar{\mu}}\sqrt{\dfrac{-\bar{z}FU_L}{2RT}}$	(T7)	$\sqrt{\dfrac{-\bar{z}FU_L}{32RT}}$	(T11)

[a] GA, good ampholyte; PA, poor ampholyte; WE, weak electrolyte; SE, strong electrolyte.

also for focusing in moving pH gradients with constant ρ. As indicated previously [14], also weak electrolytes can be focused in the moving pH gradient. For monoprotic weak electrolytes, and regarding diffusion coefficients of both separated weak electrolytes as the same, we have by insertion of Eq. (14) in Eq. (21):

$$R_{ss} = \frac{\Delta(\mathrm{pH})}{4}\sqrt{\frac{2.3\,\bar{z}\,(1-\bar{z}\,)FE}{[\mathrm{d(pH)}/\mathrm{d}x]RT}} \tag{17}$$

For weak electrolytes, we can substitute $\Delta(\mathrm{p}K_a)$ for Δ(pH), see Eqs. (T5) in Table 1.

2.2.2. Resolution in resistivity gradient with constant pH

For closely separated peaks in the resistivity gradient under the steady state, we may write:

$$\frac{\Delta\rho}{\Delta x_s} = \frac{\mathrm{d}\rho}{\mathrm{d}x} \tag{18}$$

By insertion of Eqs. (12,18) in Eq. (15) we have:

$$R_{ss} = \frac{-\Delta\rho}{4}\sqrt{\frac{\bar{\mu}I}{A\bar{D}(-\mathrm{d}\rho/\mathrm{d}x)}} \tag{19}$$

Under the steady state, we can use $-\Delta\rho/\bar{\rho} = \Delta\mu/\bar{\mu}$. Together with Eq. (9), and the relation $\bar{E} = \bar{\rho}I/A$, we obtain Eqs. (T6) in Table 1. Here, $\bar{D}$ and $\bar{E}$ are the mean diffusion coefficient and the field strength at the place of the separated pair of peaks, respectively.

2.2.3. Resolution in a combined pH and resistivity gradient

Now let us estimate steady-state resolution in a combined pH and resistivity gradient. For closely separated peaks, it holds similarly to Eq. (6):

$$\frac{\mathrm{d}\nu}{\mathrm{d}x} = \bar{\nu}\left(\frac{\Delta\mu}{\bar{\mu}\Delta x_s} + \frac{\Delta\rho}{\bar{\rho}\Delta x_s}\right) \tag{20}$$

Together with use of Eqs. (5,9,15) we have for R_{ss}:

$$R_{ss} = -\left(\frac{\mathrm{d}\mu/\mathrm{d(pH)}}{\bar{\mu}}\cdot\Delta(\mathrm{pH}) + \frac{\Delta\rho}{\bar{\rho}}\right)\sqrt{\frac{\bar{\nu}}{16\bar{D}\left(\dfrac{-\mathrm{d}\mu/\mathrm{d(pH)}}{\bar{\mu}}\cdot\dfrac{\mathrm{d(pH)}}{\mathrm{d}x} + \dfrac{-\mathrm{d}\rho}{\bar{\rho}\mathrm{d}x}\right)}} \tag{21}$$

Since the mobility is dependent on both diffusion coefficient and charge, see Nernst equation, both resistivity and pH gradient affect the resolution, see Section 3.1.

2.2.4. Resolution in zone electrophoresis

In order to see the parallels with CZE, it is useful to remember the resolution of two peaks in zone electrophoresis introduced by Giddings [32,33]. Similarly to elution separation methods it can be expressed as:

$$R_s = \frac{\Delta\nu}{4\bar{\nu}}\sqrt{\frac{\bar{\nu}L}{2\bar{D}}} \tag{22}$$

where L is the length of migration from the sampling to the detection point. With the use of the Nernst equation, Eq. (2) and the relation $U_L = -E\,L$, we obtain Eqs. (T7) in Table 1.

2.3. Peak capacity of focusing in DE with linear continuous gradients

The peak capacity was introduced by Giddings [24,31–33] as the upper limit of resolvable components for a given technique under prescribed conditions. Usually, the resolution of separated peaks is constant in the peak series and it is chosen as $R_s = 1$. It follows for the steady-state methods that the distances between neighboring peak maxima are the same and equal 4σ. Since length of the stack is L_g, the peak capacity, n, under the steady state is simply:

$$n = \frac{L_g}{4\sigma_s} \tag{23}$$

With the use of the above relationships for σ_s in discussed gradients, we can obtain the respective peak capacities, see Table 1, third column.

2.3.1. Peak capacity in a pH gradient with constant resistivity

This instance represents the well known model of focusing of good ampholytes in the stationary natural pH gradient. When the dz/d(pH) term can be regarded as the same for all separated solutes, we obtain the classical expression for peak capacity in

IEF [24,31,33] by insertion of Eqs. (2), (3), (4), (T1) into Eq. (23):

$$n = \sqrt{\frac{FEL_g\delta(\mathrm{pH})[-\mathrm{d}z/\mathrm{d}(\mathrm{pH})]}{16RT}} \tag{24}$$

where δ(pH) is the total difference in pH over the linear pH gradient of length, L_g, $\delta(\mathrm{pH}) = (\mathrm{pH})_{LE} - (\mathrm{pH})_{TE}$. Since the resistivity of the stack is regarded as constant, we can calculate the potential drop over length of the stack, U_g, as $U_g = -L_g E$, and we obtain Eqs. (T8) in Table 1. The last two equations are also applicable in a moving pH gradient [14]. As mentioned above, also weak electrolytes and poor ampholytes can be focused in a moving pH gradient. For this instance, the equation for the estimation of peak capacity can be obtained by insertion of Eq. (11) in Eqs. (T8), see Eqs. (T9) in Table 1, where $16/2.3 = 6.95-7$.

2.3.2. Peak capacity in a resistivity gradient with constant pH

For constant σ_s and $\bar{z}$ of all examined zones and the linear resistivity gradient, the $\mathrm{d}\rho/\mathrm{d}x$ term equals the ratio of the difference in resistivities, $\delta\rho$, $\delta\rho = \rho_{LE} - \rho_{TE}$, to the gradient length, $\mathrm{d}\rho/\mathrm{d}x = \delta\rho/L_g$. Together with use of Eq. (23) and Eqs. (T3), we obtain for n:

$$n = \sqrt{\frac{-L_g\bar{z}FI\delta\rho}{16ART}} \tag{25}$$

The voltage drop, U_g, over the resistivity gradient, can be obtained by integration of the local field strength, E, over gradient length, $L_g = x_{LB} - x_{TB}$.

$$U_g = -\int_{x_{TB}}^{x_{LB}} E\,\mathrm{d}x \tag{26}$$

Here, x_{LB} and x_{TB} are the moving coordinates of boundaries of the resistivity gradient with leading and terminating electrolytes, respectively. For the linear resistivity gradient, we obtain after insertion of Eqs. (3,4) in Eq. (26), integration and rearrangement:

$$U_g = \frac{\delta\rho I L_g}{2A} \tag{27}$$

By insertion of Eq. (27) in Eq. (25) and rearrangement we have Eqs. (T10) in Table 1. Eq. (25) can be modified into the forms, in which the influences of migration velocity and difference between the mobilities of LE and TE are more apparent. With the use of Eqs. (2–4,9) we can write:

$$n = \sqrt{\frac{-L_g\bar{\nu}\delta\rho}{16D_{LE}\rho_{LE}}} \tag{28}$$

In the liner resistivity gradient under the steady state, it holds for the resistivity difference with use of Eqs. (2–4):

$$-\delta\rho = \rho_{LE}\cdot\frac{\mu_{LE} - \mu_{TE}}{\mu_{TE}} \tag{29}$$

The maximum length of the stack of separated components, $L_{g,max}$ is related to the separation length, L_{sep}, and the difference in the mobilities within the stack as

$$L_{g,max} = L_{sep}\cdot\frac{\mu_{LE} - \mu_{TE}}{\mu_{TE}} \tag{30}$$

By insertion of Eqs. (29,30) into Eq. (28) we obtain for $L_g = L_{g,max}$:

$$n = \left(\frac{\mu_{LE}}{\mu_{TE}} - 1\right)\sqrt{\frac{L_{sep}\bar{\nu}}{16\,D_{LE}}} \tag{31}$$

When the background with the sample are adjusted to the LE and they form the stack of length $L_{g,max}$ within the capillary of length L, L_{sep} equals $L - L_{g,max}$ which gives with Eq. (30):

$$L_{g,max} = L\cdot\left(\frac{\mu_{LE} - \mu_{TE}}{\mu_{LE}}\right) \tag{32}$$

Further, when the constant migration velocity is maintained, the applied voltage reaches its maximum when the whole capillary is filled by the TE and $U_L = -L\,E_{TE}$. Since Eq. (25) can be modified as

$$n = \sqrt{\frac{-L_g\bar{z}FE_{TE}}{16RT}\cdot\left(\frac{\mu_{LE} - \mu_{TE}}{\mu_{LE}}\right)} \tag{33}$$

we obtain by insertion of Eq. (32) into Eq. (33) for $L_g = L_{g,max}$:

$$n = \left(1 - \frac{\mu_{TE}}{\mu_{LE}}\right)\sqrt{\frac{-\bar{z}FU_L}{16RT}} \tag{34}$$

2.3.3. Peak capacity in zone electrophoresis

When the background with neither resistivity nor conductivity gradient is used, we arrive at the separation by zone electrophoresis. For the peak capacity in zone electrophoresis we have the classical expression [31–33], see Eqs. (T11) in Table 1.

3. Discussion

When appropriate, the variables in above equations should be treated as vector quantities, namely, μ, z, $\Delta(\mathrm{pH})$, I, E, $(-U)$ and $\mathrm{d(pH)}/\mathrm{d}x$ are negative for focusing of anions and positive for focusing of cations, respectively; $\mathrm{d}\mu/\mathrm{d(pH)}$, $\mathrm{d}z/\mathrm{d(pH)}$ and $\Delta\rho$ are always negative.

Through the theoretical part, the approximation, $\nu \sim \bar{\nu}$, and similar ones were used several times. Let us estimate the magnitude of error of such an approximation for the calculation of parameters of single peak and that of pair of closely separated peaks. The error can be visualized as the percentage of relative change of ν over the length of one σ_s, $\xi\%$. In a linear gradient of ν, it is $\xi\% = 100\sigma_s(\mathrm{d}\nu/\mathrm{d}x)/\bar{\nu}$, see Fig. 1. With the use of Eq. (5), it is $\xi\% = 100D/(\sigma_s \cdot \bar{\nu})$. Since the expected σ_s is $\sigma_s > 0.1$ mm, $D = 5 \cdot 10^{-4}$ mm^2 s^{-1} or lower and $\bar{\nu} > 0.1$ mm s^{-1}, $\xi\%$ is $\xi\% < 5\%$. With the use of the above relations, it can be shown that the relative change in other variables over the peak width is similar. It was mentioned previously [26] that change in the conductivity by several % within the zone still allows us to approximate the zone by the Gaussian curve. Thus, the derived equations can reasonably be used for the estimation of characteristics of discussed modes of electrophoresis, see below.

3.1. Comparison of the separation power of ITP with conductivity gradient with other electrophoretic techniques

Let us estimate the separation power of the discussed methods expressed in terms of n close to upper limits which is given by the usable voltage. It is chosen as $U_L = 20$ kV. The typical value of the L/L_g ratio is $L/L_g = 4$ in focusing with a moving pH gradient. Further, let us take $\delta(\mathrm{pH}) = 6$ and $-\mathrm{d}z/\mathrm{d(pH)} = 5$ as typical values for proteins. We obtain $n = 610$ from Eqs. (T8) assuming $U_g = U_L/4$. For weak electrolytes in a pH gradient, the maximum of n is at $\bar{z} = 0.5$. When we take $\delta(\mathrm{pH}) = 6$ again, we have $n = 210$ from Eqs. (T9). Eq. (34) is convenient for the estimation of n in focusing of strong electrolytes in the moving resistivity gradient. When we take the ratio $\mu_{\mathrm{LE}}/\mu_{\mathrm{TE}} = 4$, we obtain $n = 167$ with $-zU_L = 20$ kV. For the voltage drop chosen above, we have $n = 158$ for zone electrophoresis from Eqs. (T11).

By comparison of calculated peak capacities, the highest n should be achievable for focusing of proteins in the pH gradient where n is about three times higher than n for poor ampholytes and weak electrolytes. However it was found [34] that, in the same focusing run, low molecular ampholytes with $-\mathrm{d}z/\mathrm{d(pH)}$ lower than unity [35] have their zone width comparable or even lower than that of cytochrome C, myoglobin or hemoglobin which have a $-\mathrm{d}z/\mathrm{d(pH)}$ term larger by one order of magnitude. Though it could be partly explained by the possible nonlinearity of the pH gradient, probably other disturbing effects are responsible for the increase in the zone width of the proteins.

It follows from the above discussion that the separation power of electrofocusing variants is similar to that of CZE. This conclusion is well known from several previous theoretical treatments [24,30,31,33]. Here, the interesting finding is that both weak and strong electrolytes as well as ampholytes could be focused in a continuous resistivity gradient with the separation power comparable to both focusing of ampholytes and weak electrolytes in a pH gradient and to zone electrophoresis. The basic variable is effective charge of the analyte; higher $\bar{z}$ means a narrower peak. When we consider two closely separated analytes with similar $\bar{\mu}$, the analyte with higher $\bar{z}$ and lower D should give the narrower zone.

Recently, the separation power of ITP of strong electrolytes under the condition of generation of square wave zones was estimated [36]. The maximum number of separable square wave zones was calculated as equal to 30 for $\bar{\nu} = 5 \cdot 10^{-4}$ m s^{-1}, $\mu_{\mathrm{LE}} = 80 \cdot 10^{-9}$ m^2 V^{-1} s^{-1}, $\mu_{\mathrm{TE}} = 20 \cdot 10^{-9}$ m^2 V^{-1} s^{-1}, $L_{\mathrm{sep}} = 0.2$ m and the resolution defined as $(L_{\mathrm{A}} - W_{\mathrm{AB}})/L_{\mathrm{A}}$ equals 0.9. Here, L_{A} and W_{AB} are the length of the steady-state zone of component A

and the width of the steady-state boundary between components A and B, respectively. When we take such values of mobilities, separation length and isotachophoretic velocity for calculation of the separation power of focusing in a continuous resistivity gradient, we obtain $n = 168$ from Eq. (32). Since the number of separable zones is dependent on the definition of the extent of the separation [30,36], the lower n in the former case could be explained mainly by the fact that in ITP of square wave zones, a lower extent of mutual mixing of neighboring zones in comparison to Gaussian zones is needed for the reliable detection of resolved zones.

In the general case of focusing in combined pH and resistivity gradient, the separation window is framed by the difference in pH values and the conductivities of LE and TE, respectively. Then, σ_s can be smaller or larger than that in single pH or resistivity gradients, depending on relative magnitude and the direction of pH and conductivity gradients in connection with analyte D and $dz/d(pH)$ terms, see Eq. (22). Firstly, the influence of respective gradient is proportional to its steepness, i.e., to the difference in pH or resistivity over gradient length. As shown in the following paragraph, the relative steepness of both gradients can be simply controlled by the composition of the leading electrolyte. In this way, the chance for separation can be modified. Secondly, the influence of respective gradient is dependent on the ionic state of analyte, namely its $\bar{z}$ and $dz/d(pH)$ terms. For example, in the combined pH and ρ gradient, only ρ gradient is effective for focusing of strong electrolytes which have $dz/d(pH) = 0$.

3.2. Generation of pH and conductivity gradients

In Section 2, the possibility of the generation of either pH gradient with constant ρ or resistivity gradient with constant pH was assumed. A question may arise as to whether such single moving gradients are also possible to obtain in a non-ampholyte background. In order to visualize the pH and resistivity profile in a moving stack of carriers, let us model the background by the series of equal and equidistant zones of monoprotic electrolytes. In such an instance, the pH and resistivity within the zones can be calculated by Beckers' procedure [1,37] modified for Personal Computer. The pH and resistivity course in Fig. 2a was calculated for the series of weak anions with equal ionic mobilities and equidistant pK_a values, see Table 2. The composition of LE was chosen so that ρ within the obtained pH gradient can be regarded as constant, at least in its central part. The focusing of ampholytes and weak electrolytes in such a gradient can be reasonably approximated by Eqs. (T1), (T4), (T8) and Eqs. (T2), (T5), (T9), respectively.

The profiles in Fig. 2b are related to the model of the moving stack of strong electrolytes with gradually decreasing ionic mobilities, see Table 3. Unlike the previous figure, there is a pronounced linear resistivity gradient with the almost constant pH. Eqs. (T3), (T6), (T10) are appropriate for description of the focusing in such a gradient.

In Fig. 2c, the pH and resistivity profiles were calculated for the same compounds as in Fig. 2a, only the pH of LE was chosen to be more acidic, see Table 4, so that the considerable resistivity gradient is superposed to the pH gradient. Though the peak capacity in such gradient cannot be generally calculated, the peak variances and the resolution of a pair of closely separated peaks can be approximated by Eqs. (14,21), respectively. Nevertheless, when only strong electrolytes are focused in such a combined gradient, Eqs. (T3), (T6), (T10) can be used for the description of the separation power similarly as in the gradient generated by a series of strong electrolytes.

In ITP with a moving stack of carrier ampholytes, approximately linear profiles of both pH and ρ are usually observed [1,19–22]. In some instances, the pH difference between LE and TE is about one pH unit or less while the difference in ρ amounts up to one order of magnitude [1,20–22]. Thus, the considerable influence of the resistivity gradient on the separation and focusing is to be expected.

There is experimental evidence [21] that strong electrolytes can be focused in a moving stack of carrier ampholytes. It follows from the discussion above, that the stack of either weak or strong electrolytes can be used as the background for the focusing of the strong electrolytes as well as of weak electrolytes and ampholytes into the separated Gaussian zones. While there is a good experience with now currently available carrier ampholytes, their

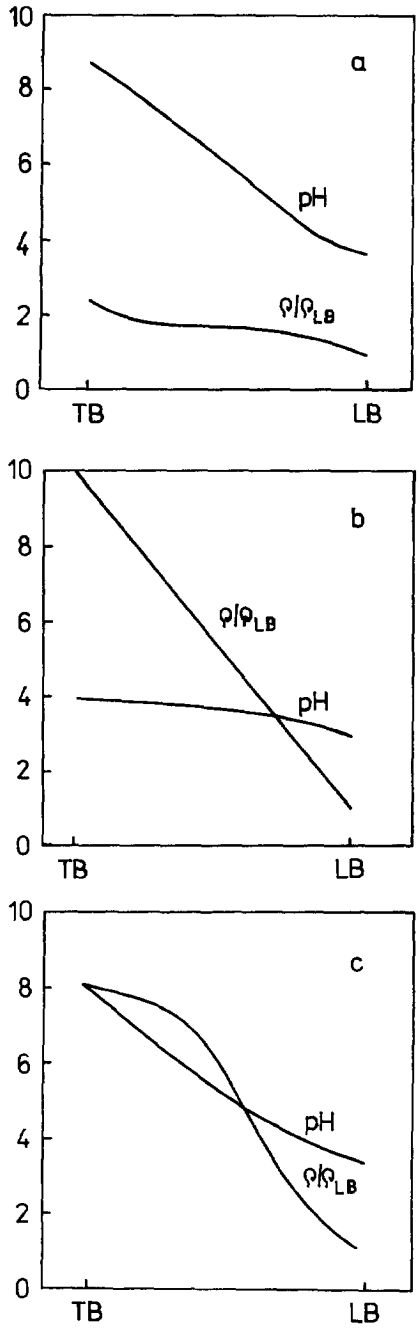

Fig. 2. pH and resistivity profiles within the moving stack of equal and equidistant zones calculated by Beckers' procedure [1,37]. LB and TB = boundary between the stack and the leading and terminating electrolyte, respectively; (a) moving stack of anions of monoprotic weak acids with equal ionic mobilities and uniformly spaced pK_a values, for the selected values see Table 2; (b) moving stack of anions of monoprotic strong acids, for selected values see Table 3, (c) as (a), with a different pH of LE, see Table 4.

Table 2
Selected values from pH and resistivity profile in moving stack of anions of weak acids.

Component		Zone		
$-\mu_0$ (10^{-9} m^2 V^{-1} s^{-1})	pK_a	$-\bar{z}$	pH	ρ/ρ_L
30	3	0.80	3.60	1.00
30	4	0.59	4.16	1.36
30	5	0.50	5.00	1.60
30	6	0.49	5.97	1.65
30	7	0.48	6.97	1.67
30	8	0.45	7.91	1.78
30	9	0.33	8.69	2.43

Concentration and pH of leading component are 0.01 mol l^{-1} and 3.60, respectively. Counterion μ_0 and pK_a are $30 \cdot 10^{-9}$ m^2 V^{-1} s^{-1} and 9.0, respectively.

Table 3
Selected values from pH and resistivity profile in moving stack of anions of strong acids.

Component		Zone		
$-\mu_0$ (10^{-9} m^2 V^{-1} s^{-1})	pK_a	$-\bar{z}$	pH	ρ/ρ_L
40.0	<-3	1.0	3.00	1.00
20.0	<-3	1.0	3.28	2.00
13.3	<-3	1.0	3.45	3.01
10.0	<-3	1.0	3.57	4.00
8.00	<-3	1.0	3.66	5.00
6.67	<-3	1.0	3.74	6.01
5.70	<-3	1.0	3.81	7.02
5.00	<-3	1.0	3.86	8.00
4.44	<-3	1.0	3.91	9.01
4.00	<-3	1.0	3.96	10.0

Concentration and pH of the leading component are 0.01 mol l^{-1} and 3.0, respectively. Counterion μ_0 and pK_a are $30 \cdot 10^{-9}$ m^2 V^{-1} s^{-1} and 9.0, respectively.

Table 4
Selected values from pH and resistivity profile in moving stack of anions of weak acids

Component		Zone		
$-\mu_0$ (10^{-9} m^2 V^{-1} s^{-1})	pK_a	$-\bar{z}$	pH	ρ/ρ_L
30	3	0.67	3.30	1.00
30	4	0.37	3.77	1.79
30	5	0.20	4.36	3.35
30	6	0.12	5.13	5.60
30	7	0.092	6.01	7.22
30	8	0.087	6.98	7.66
30	9	0.082	7.95	8.11

Concentration and pH of leading component are 0.01 mol l^{-1} and 3.30, respectively. Counterion μ_0 and pK_a are $30 \cdot 10^{-9}$ m^2 V^{-1} s^{-1} and 9.0, respectively.

optical transparency in the UV range under 260 nm is limited. Thus, there is a possible field for improvement in the development of the background dedicated to the focusing in the combined continuous pH and resistivity gradient.

In most of the previously described experiments with the focusing of analytes in the background generated by the moving stack of carrier ampholytes, the considerable resistivity gradients are superposed on the pH gradients. Based on equations derived, the resistivity gradient can substantially modify the separation in comparison to expectation based on pH gradient with constant conductivity.

4. Conclusions

It follows from equations derived that the separation power of the focusing in the resistivity gradient can be comparable to that of IEF and CZE. The high separation power of ITP with continuous pH and resistivity gradients was shown previously (e.g., Refs. [8,19,21]). According to the equations derived, such a mode of focusing could be used for all ionisable analytes including strong and weak electrolytes as well as good and poor ampholytes. It may be useful to use the term ITF for all modes discussed above though this term was suggested [29] for the isotachophoretic separation of proteins in a polyampholyte background with a field strength gradient. The advantage of the focusing in the combined pH and resistivity gradient can be seen, similarly to other focusing methods, in its focusing ability, i.e., in the capability to increase the concentration at the detection place relative to the concentration in the sample. In addition to lower demands on the sampling technology and the better use of the sample, it mainly means a higher analyte concentration available for detection. In the above discussed example of focusing, expected σ_s is about 0.1 mm. Since L_g is comparable to the length of the sampled solution, which may be up to 100 mm, an increase in the concentration by at least by two orders of magnitude can be expected. In comparison with a CZE–ITP combination, the peaks in continuous gradients are focused at the positions, where the effective mobility of the analyte matches the effective mobility of the background which supports the peak symmetry. Thus, the problems with sample overloading may be reduced.

In comparison with IEF, analytes in moving pH and resistivity gradients are appreciably dissociated so that no problems arise with their mobilization and the migration velocity can be comparable to that in CZE. Also, due to the appreciable charge of the same sign, the aggregation of separated macromolecules may be reduced.

5. List of symbols, abbreviations and subscripts

5.1. Symbols

A	Capillary cross section (m^2)
c_m	Concentration in peak maximum ($mol\ l^{-1}$)
D	Diffusion coefficient ($m^2\ s^{-1}$)
D^*	Effective dispersion coefficient ($m^2\ s^{-1}$)
E	Electric field strength ($V\ m^{-1}$)
F	Faraday constant (96 487 A s equiv^{-1})
I	Electric current (A)
L	Length of capillary from sampling to the detection point (m)
L_g	Length of the moving gradient (m)
$L_{g,max}$	Maximum length of the moving gradient (m)
n	Peak capacity
pI	Isoelectric point
R	Gas constant (8.314 V A s K^{-1} equiv^{-1})
R_s	Resolution
R_{ss}	Steady-state resolution
t	Time (s)
T	Thermodynamic temperature (K)
U_L	Electric potential difference over L (V)
U_g	Electric potential difference over L_g (V)
v	Local migration velocity of component ($m\ s^{-1}$)
$\bar{v}$	Isotachophoretic velocity ($m\ s^{-1}$)
V_g	Volume of natural pH gradient (m^3)
x	Moving length coordinate, the distance from peak center (m)
y	Length coordinate along the capillary axis (m)
z	Effective charge
δ	Difference of variable over gradient length
Δ	Difference of variable between two closely separated peaks
κ	Electric conductivity ($A\ V^{-1}\ m^{-1}$)

μ	Effective mobility ($m^2 V^{-1} s^{-1}$)
μ_0	Ionic mobility ($m^2 V^{-1} s^{-1}$)
ρ	Electric resistivity ($V m A^{-1}$)
σ	Actual length based standard deviation of Gaussian zone (m)
σ_s	Steady-state length based standard deviation of Gaussian zone (m)
σ^2	Length based variance of Gaussian zone (m^2)
σ_s^2	Steady-state length based variance of Gaussian zone (m^2)

5.2. Abbreviations

CZE	Capillary zone electrophoresis
DE	Displacement electrophoresis
DNA	Desoxyribonucleic acid
GA	Good ampholyte
IEF	Isoelectric focusing
ITF	Isotachophoretic focusing
ITP	Isotachophoresis
LB	Boundary between LE and moving gradient
LE	Leading electrolyte
PA	Poor ampholyte
SE	Strong electrolyte
TE	Terminating electrolyte
TB	Boundary between TE and moving gradient
WE	Weak electrolyte

5.3. Subscripts

LB	Boundary between LE and moving gradient
LE	Leading electrolyte
TB	Boundary between TE and moving gradient
TE	Terminating electrolyte
s	Steady state
g	Moving gradient
max	Maximum value

5.4. Superscript

	Mean value of variable within the peak, mean value of variable of closely separated peaks

Acknowledgments

This work was supported by a grant of the Academy of Sciences of the Czech Republic No. A 4031504.

References

[1] F.M. Everaerts, J.L. Beckers and T.P.E.M. Verheggen, Isotachophoresis, Elsevier, Amsterdam, 1976.
[2] P. Boček, M. Deml, P. Gebauer and V. Dolník, Analytical Isotachophoresis, VCH, Weinheim, 1988.
[3] W. Thormann, Sep. Sci., 19 (1984) 455.
[4] W. Thormann and R.A. Mosher in A. Chrambach, M.J. Dunn and B.J. Radola (Editors), Advances in Electrophoresis, Vol. 2, VCH, Weinheim, 1988, p. 45.
[5] R.A. Mosher, D.A. Saville and W. Thormann, The Dynamics of Electrophoresis, VCH, Weinheim, 1992.
[6] A.J.P. Martin and F.M. Everaerts, Anal. Chim. Acta, 38 (1967) 233.
[7] S. Hjertén, Electrophoresis, 11 (1990) 665.
[8] S. Hjertén and M. Kiessling-Johansson, J. Chromatogr., 550 (1991) 811.
[9] L. Křivánková, P. Gebauer and P. Boček, J. Chromatogr. A, 716 (1995) 35.
[10] F. Foret, E. Szökö and B. Karger, J. Chromatogr., 608 (1992) 3.
[11] T. Hirokawa, A. Ohmori and Y. Kiso, J. Chromatogr., 634 (1993) 101.
[12] D. Kanianský, F. Ivanyi and F. Onuska, Anal. Chem., 66 (1994) 1817.
[13] D.S. Stegehuis, U.R. Tjaden and J. van der Greef, J. Chromatogr., 591 (1992) 341.
[14] K. Šlais, J. Microcol. Sep., 5 (1993) 469.
[15] S. Hjertén and M. Zhu, J. Chromatogr., 346 (1985) 265.
[16] S. Hjertén, J. Liao and K. Yao, J. Chromatogr., 387 (1987) 127.
[17] S. Hjertén, K. Elenbring, F. Kilár, J.L. Liao, A.J.C. Chen, C.J. Siebert and M.D. Zhu, J. Chromatogr., 403 (1987) 47.
[18] C. Schwer, Electrophoresis, 16 (1995) 2121.
[19] F. Acevedo, J. Chromatogr., 470 (1989) 407.
[20] T. Manabe, H. Yamamoto and T. Okuyama, Electrophoresis, 10 (1989) 172.
[21] H. Yamamoto, T. Manabe and T. Okuyama, J. Chromatogr., 480 (1989) 331.
[22] T. Izumi, T.Nagahori and T. Okuyama, J. High Resolut. Chromatogr., 14 (1991) 351.
[23] H. Svensson, Acta Chem. Scand., 15 (1961) 325.
[24] J.C. Giddings and H. Dahlgren, Sep. Sci. Technol., 6 (1971) 345.
[25] M. Almgren, Chem. Scr., 1 (1971) 69.
[26] K. Šlais, J. Chromatogr. A, 684 (1994) 149.
[27] K. Šlais, J. Microcol. Sep., 7 (1995) 127.
[28] K. Šlais, J. Chromatogr. A, 730 (1996) 247.

[29] R. Charlionet, A. Bringard, Ch. Davrinche and M. Fontaine, Electrophoresis, 7 (1986) 558.
[30] K. Šlais, J. Chromatogr. A, 679 (1994) 335.
[31] J.C. Giddings, Unified Separation Science, Wiley, New York, 1991.
[32] J.C. Giddings, Sep. Sci., 4 (1969) 181.
[33] J.C. Giddings, Anal. Chem., 53 (1981) 945A.
[34] J. Caslavska, S. Molteni, J. Chmelík, K. Šlais, F. Matulík and W. Thormann, J. Chromatogr. A, 680 (1994) 549.
[35] K. Šlais and Z. Friedl, J. Chromatogr. A, 661 (1994) 249.
[36] P. Gebauer and P. Boček, Electrophoresis, 16 (1995) 1999.
[37] J.L. Beckers and F.M. Everaerts, J. Chromatogr., 68 (1972) 207.